JBC Papers in Press. Published on July 31, 2017 as Manuscript M117.795286
The latest version is at http://www.jbc.org/cgi/doi/10.1074/jbc.M117.795286

Ascorbate peroxidase proximity labeling coupled with biochemical fractionation identifies promoters of endoplasmic reticulum–mitochondrial contacts

Il-Taeg Cho[1], Guillaume Adelmant[2], Youngshin Lim[1], Jarrod A Marto[1,2], Ginam Cho[1], and Jeffrey A. Golden[1]*

[1]Department of Pathology, Brigham and Women's Hospital, Harvard Medical School, Boston, MA 02115; [2]Department of Cancer Biology, Department of Pathology and Blais Proteomics Center, Dana-Farber Cancer Institute, Harvard Medical School, Boston, MA.

Running title: RTN1A promotes ER-mitochondria contacts

*To whom correspondence should be addressed: Jeffrey Golden, Department of Pathology, Brigham & Women's Hospital, Harvard Medical School, 75 Francis Street Boston, MA 02115
Email: jagolden@bwh.harvard.edu

Key words: Engineered ascorbate peroxidase (APEX), Interorganelle communication, ER-mitochondria contacts (EMCs), RETICULON (RTN).

ABSTRACT

To maintain cellular homeostasis, subcellular organelles communicate with each other and form physical and functional networks through membrane contact sites (MCS) coupled by protein tethers. In particular, endoplasmic reticulum (ER)-mitochondria contacts (EMC) regulate diverse cellular activities such as metabolite exchange (Ca^{2+} and lipids), intracellular signaling, apoptosis and autophagy. The significance of EMCs have been highlighted by reports indicating that EMC dysregulation is linked to neurodegenerative diseases. Therefore, obtaining a better understanding of the physical and functional components of EMCs should provide new insights into the pathogenesis of several neurodegenerative diseases. Here we applied engineered ascorbate peroxidase (APEX) to map the proteome at EMCs in live HEK293 cells. APEX was targeted to the outer mitochondrial membrane, and proximity-labeled proteins were analyzed by stable isotope labeling with amino acids in culture (SILAC)-LC/MS-MS. We further refined the specificity of the proteins identified by combining biochemical subcellular fractionation to the protein isolation method. We identified 405 proteins with a 2.0-fold cut-off ratio (log base 2) in SILAC quantification from replicate experiments. We performed validation screening with a Split-Rluc8 complementation assay that identified RETICULON1A (RTN1A), an ER-shaping protein localized to EMCs as an EMC promoter. Proximity mapping augmented with biochemical fractionation and additional validation methods reported here could be useful to discover other components of EMCs, identify mitochondrial contacts with other organelles, and further unravel their communication.

INTRODUCTION

Interorganelle communication has emerged as a critical physiologic function required to maintain cellular homeostasis. The functional interplay between cellular organelles is mediated through the membrane contacts formed by protein tethers within the membranes of the two organelles holding them in close proximity (1-4). Different forms of membrane contacts display a wide variety of functions depending on the organelles involved and the types of membrane contacts. For instance, the endoplasmic reticulum and mitochondria contacts (EMC) are the hub for Ca^{2+} exchange, phospholipid exchange, autophagy, mitochondrial biogenesis, and ER stress response (5-10). At ER-Plasma membrane junctions, in addition to Ca^{2+} and lipid transport, cell signaling regulation and ER shaping occurs (11-13). Bi-directional lipid trafficking and secretion of proteins are well known to occur at the point of ER and Golgi juxtaposition (14-16). In yeast, mitochondrial attachments to plasma membranes are important for mitochondrial fission and partitioning in cell division (17,18).

Membrane contacts are established by interactions between proteins presented on the outer surface of each organelle, allowing subdomains of membranes to appose each other within 10 nm to 50 nm but without fusion (1,3,19). Likely due to their important roles in cellular homeostasis, defects in regulation of these contacts, have been linked to several human diseases. For example, overexpression of Familial Alzheimer's Disease (FAD) associated presenilin 2 mutations significantly increase EMCs and causes an imbalance of intracellular Ca^{2+} homeostasis (20,21). Overexpression of hereditary spastic paraplegia-associated *REEP1* mutations impairs the level of ER-mitochondria contacts and results in neuritic degeneration in cortical neurons (22). Missense mutation (P56S) in the integral ER membrane protein vesicle-associated membrane protein-associated protein B (VAPB) has been linked to atypical amyotrophic lateral sclerosis (ALS8). P56S mutations impair ER-Golgi vesicle trafficking and perturb Ca^{2+} handling by ER-mitochondria contacts formed by VAPB and outer mitochondrial membrane proteins like protein tyrosine phosphatase-interacting protein 51 (PTPIP51)(23-25). Another example is BAP31. This multifunctional protein forms an apoptosis platform with Fission 1 homologue (Fis1) at ER-mitochondria contacts, controls quality of newly synthesized proteins in the ER, and regulates TCR signaling for T cell activation. Mutations in BAP31 have been linked to X-linked intellectual disabilities with severe phenotypes such as deafness, dystonia, congenital microcephaly (26-29). Finally, dysregulation of EMCs, resulting from mutations in various proteins participating in contact between these two organelles, has been extensively linked to neurodegenerative diseases. (30-34).

Understanding the cellular physiology and underlying mechanisms governed by interorganelle communication is crucial to gain new insights into potential therapeutic opportunities. Unfortunately, no well-defined screening assay existed in mammalian cells. Although genetic screening has been fruitful in identifying EMCs in yeast, both similarities and differences exist in mammalian cells. For instance, components of the ER-mitochondria encounter structure (ERMES) complex in yeast were identified and characterized through a genetic screen in which lethal mutant strains were isolated by expressing synthetic ER-mitochondria bridge protein (35). The ERMES

complex was found to be composed of ER membrane protein (Mmm1), two outer mitochondrial membrane proteins (Mdm10, Mdm34) and a cytosolic protein (Mdm12) (35-37). Unfortunately, none of the orthologs of ERMES complex has been identified in mammalian cells. Herein we have developed a systematic approach to identify protein components associated with EMCs in mammalian cells.

To identify proteins that coordinate EMCs, we have adopted the proximity labeling technique using engineered ascorbate peroxidase (APEX). APEX-mediated labeling, has proven to be a powerful tool for labeling proteins in live cells (38). It has been successfully used to map the proteome of the mitochondrial intermembrane, ER-PM junctions, and proteome of primary cilia (13,39-43). To capture proteins associated with EMCs, we fused a mitochondria targeting sequence to APEX and expressed it in HEK293 cells. We utilized SILAC-based quantitative LC-MS/MS to identify proteins enriched following APEX labeling. We identified 405 proteins across two independent replicates, including RETICULON1A (RTN1A), an ER shaping protein localized to EMC. We further validated that RTN1A function in EMC using a live cell assay. All together we have characterized a new function for RTN1A and we have defined a method to identify proteins important in inter-organelle contacts. These data provide new insights into several human diseases and new potential targets for therapy.

RESULTS

Targeted expression of APEX to mitochondrial outer membrane (Mit-APEX)

To identify potential target proteins associated with ER-mitochondria contacts we used the experimental scheme depicted in Figure 1A. Mit-APEX cannot label ER proteins when the respective membranes are separated by more than approximately 20 nm (41,44,45). At EMC sites, both ER and mitochondrial proteins will be labeled (Fig.1A, contact). In contrast, when ER and mitochondrial members are not juxtaposed, the APEX system only labels mitochondrial proteins (Fig. 1A, no contact). We thus anticipate the proteins identified will include not only ER-mitochondria tethering proteins but also ER and mitochondrial proteins that are not directly engaged in EMC but may still play a functional role.

pcDNA3.1-Mit-APEX was transfected in HEK293 cells and protein expression was determined to be stable (Fig. 1B). A single band was detected by western blot when probed with an α-flag antibody indicating strong expression and no obvious degradation products. Next we confirmed the mitochondrial localization of Mit-APEX. Mit-APEX expressed in HeLa cells showed clear localization to mitochondria as assayed by overlapping expression between FLAG (Mit-APEX) and TOM20 (a subunit of the outer mitochondrial membrane protein complex) (Fig. 1C). Finally, we examined the biotinylation activity of Mit-APEX. Proximity labeling was done essentially as previously described (41). Whole cell lysates obtained from HEK293 cells expressing Mit-APEX were subjected to SDS-PAGE and biotinylated proteins were probed with streptavidin-HRP. In the absence of Mit-APEX, no biotin labeling was detected (Fig. 1D, lanes 1 and 2). However, in the presence of Mit-APEX and the biotin substrate (but not in the absence of this substrate), strong biotinylation was present (Fig. 1D, lanes 3 and 4). Moreover we

compared our Mit-APEX targeted to outer mitochondrial membrane with APEX expressed in the mitochondrial matrix (41); they showed distinctive biotinylation patterns indicating specificity to the Mit-APEX targeting (data not shown). Finally, we performed pilot proximity labeling to know whether Mit-APEX can label known ER-mitochondria tethers, Inositol 1,4,5'-triphosphate receptor II (IP3RII) calcium channel, vesicle-associated membrane protein-associated protein B (VAPB) and B-cell receptor-associated protein 31 (BAP31). As predicted, Mit-APEX labeled those ER-mitochondria tethering proteins, which is likely at EMCs. Taken together, these data indicate we successfully targeted an active and stable form of APEX to the outer mitochondrial membrane, and it is suitable for mapping proteins at EMCs.

Purification of proteins proximity-labeled by Mit-APEX after SILAC and biochemical subcellular fractionation

To facilitate the identification of proteins labelled by APEX at the ER-mitochondria interface, we adopted a quantitative LC-MS/MS approach relying on stable isotope labeling with amino acids in culture (SILAC)(46-48). HEK293 cells were equilibrated in light or heavy isotope containing medium for a minimum of five passages, with the efficiency of isotope incorporation assessed by mass spectrometry (See Fig. 2A for experimental protocol). Excess proline was used as a supplement (200 mg/L) to prevent the metabolic conversion of heavy arginine to heavy proline (49). Cell cultures equilibrated in SILAC media were either mock transfected (SILAC-light) or transfected with pcDNA3.1-Mit-APEX (SILAC-heavy). An independent biological replicate with a reverse labeling strategy was also prepared. After labeling with heavy amino acids, proximity labeling by Mit-APEX was performed as described in the materials and methods, then the microsomal fraction, containing ER, was isolated from cells by differential centrifugation, the biotinylated proteins recovered from the microsomal fractions by releasing them from streptavidin-magnetics beads, and this was followed by LC/MS-MS analysis (Fig. 2A). Western blotting after biochemical fractionation validated that most proteins from the cytosol (Tubulin) and nucleus (TCF7L2) were removed, whereas ER proteins (Calnexin) and some mitochondrial proteins (ATP5A) were retained (Fig. 2B). We next compared biotinylation patterns in each fraction and found a nice separation of microsomal fractions and biotinylated proteins (Fig. 2B, Streptavidin-HRP). As a final quality control step prior to mass spectrometry analysis, a separate protein purification was performed from control and experimental samples and eluted proteins were subjected to SDS-PAGE/silver staining (Fig. 2C).

Proximity labeling by Ascorbate Peroxidase (APEX) identified RTN1A as a promoter of ER-Mitochondrial contacts

Mass spectrometry identified approximately 1,100 proteins that were common to experiment 1 (control cultured in light isotope, Mit-APEX in heavy isotope) and experiment 2 (control cultured in heavy isotope, Mit-APEX in light isotope). To further identify significantly enriched proteins, we analyzed SILAC results based on fold enrichment ratios instead of comparing abundance among proteins because the absolute level of proximity-labeled proteins is dependent on the

numbers of tyrosine residues accessible by biotin phenol radicals. To determine cut-off ratio, we normalized both replicates using quantile normalization method in R (RStudio Team (2015). RStudio: Integrated Development for R. RStudio, Inc., Boston, MA URL http://www.rstudio.com/). Cut-off ratios was determined by the fold change of IP3Rs (2.0 of log base 2), a known EMC tether. Applying a 2.0-fold cut-off ratio (log base 2), we identified 405 overlapping proteins in the two experiments (Table 1). A gene ontology (GO) analysis was performed using Functional Enrichment analysis tool, Funrich (50). For GO term cellular component (CC) definitions, the top 15 clusters (p-value < 0.05) are reported (Fig. 3B).

In the CC, cytoplasmic (66.3%) cluster was omitted and sub-terms were presented to show greater specificity of the results (Fig. 3). In total, 88 proteins were annotated to ER by Funrich (Table 1). Among the proteins, we identified Inositol 1,4,5'-triphosphate receptor II (IP3RII) calcium channel, vesicle-associated membrane protein-associated protein B (VAPB) and B-cell receptor-associated protein 31 (BAP31), each well-known ER-Mitochondria tethers. The presence of the tethers in our screen were confirmed by western blotting (Fig. 4B).

The ATLASTIN (ATL2) and RETICULON (RTN1, RTN3) ER-shaping proteins were identified as interesting novel targets because of their known role in regulating ER structure which is likely critical in forming EMCs. Furthermore, a study in yeast showed ER-shaping proteins facilitate lipid transfer from ER to mitochondria, which occurs at EMCs (51). When Fold changes in SILAC are compared, RTN1A (2.7 fold increase), was higher than the known EMC tether IP3RII (2.0 fold in replicates 1 and 2) and VAPB (2.3 fold). For all of these reasons we chose RTN1A was an important protein to study.

The coordinated action of ATLs and RTNs is important for forming and stabilizing tubular ER-structure (52-55). However, little is known regarding their role in EMCs in mammals. To test whether ATLs and RTNs affect ER-mitochondria contact, we used our Split Rluc8 complementation assay to test ATLs and RTNs (Fig. 4A). Notably, RTN1A created a 4.4 fold increase in ER-Mitochondria contacts (Fig. 4D), but no change was observed with ATLs (data not shown). RTN2B (2.5 fold) and RTN3B (1.3 fold) showed small but statistically significant fold increases in EMCs. Taken together, these results indicate RTN1A has a role in forming ER-mitochondria contacts.

Interestingly, we noticed that RTN1A, which has a longer N-terminus than the other RTN family members RTN1C, RTN2B, and RTN3B, showed higher Split-Rluc8 activity (ER-mitochondria contacts, Fig. 4C and D). We postulated that the N-terminus of RTN1A might have an important role in ER-mitochondria contacts. To test this, we used N-terminal (1-568 a.a) deletion construct of RTN1A (RTN1A-ΔN568) and a N-terminus of RTN1A (1-568 a.a)-RTN3B fusion construct (RTN1A-N568-RTN3B). The N-terminal deletion construct of RTN1A showed minimal activity, whereas the RTN1A-RTN3B fusion construct increased EMCs (Fig. 4C and E). Consistent with the split-Rluc8 complement assay results, N-terminal deletion of RTN1A significantly reduced the level of biotin labeling by Mit-APEX, but full length RTN1A was enriched (Fig. 4F). These data indicate the N-terminus of RTN1A is critical for this activity but it does require the C-terminus from a RTN family member.

DISCUSSION

The cell's cytoplasm is tightly packed with organelles, macromolecules and small molecules (56,57). Communication between the organelles is highly orchestrated and essential for normal cellular homeostasis (1-3,58). Indeed, a growing body of evidence indicates that a defect in inter-organelle communication may play a role in the pathogenesis of multiple human diseases (30,33,59,60). More specifically, abnormalities associated with EMCs have been reported to be linked to multiple neurodegenerative disorders (20,30,61). However, the pathologic mechanisms underlying these disorders remain to be fully clarified. Identifying the full repertoire of proteins regulating ER-mitochondria contacts and understanding molecular events occurring between ER and mitochondrial contacts are critical to developing potential therapeutic strategies.

In this study, we applied proximity labeling using engineered ascorbate peroxidase (APEX) to identify proteins that exist within ER-mitochondrial contacts. The short half life (< 1 ms) and small labeling radius (< 20 nm) of the biotin-phenoxyl radical converted by APEX, enable capture of proteins located in close proximity in live cells (13,39-43). To capture proteins associated with ER-mitochondria contacts, we targeted APEX to the outer mitochondrial membrane in HEK293 cells, enriched the microsomal fraction and purified biotyinylated proteins using Streptavidin-magnetic beads. Although proximity labeling by APEX is highly specific, a combination of SILAC labeling and biochemical purification improved the specificity of targets identified by proximity labeling, particularly when APEX is exposed to the outside of membrane-enclosed cellular compartments. Indeed, inclusion of a fractionation step removed a large portion of cytosolic, nuclear, and mitochondrial biotinlyated proteins (see Fig. 2B).

LC-MS/MS analysis identified 405 proteins overlapping from replicate experiments with a cut-off ratio 2.0 (log base 2). In total 88 proteins were annotated to the ER by Funrich (Table 1). Identification of Inositol 1,4,5'-triphosphate receptor II (IP3RII) calcium channel, vesicle-associated membrane protein-associated protein B (VAPB) and B-cell receptor-associated protein 31 (BAP31), all well-known ER-Mitochondria tethers, demonstrated the robustness of our approach (Table 1 and Figure 4B). Unexpectedly, we did not identify mitofusin 2 (MFN2), which is known to participate in EMC. It is possible electron-rich residues such as tyrosine in MFN2 might not be accessible by phenoxyl radical. For instance, the electron rich residues could be masked by interacting proteins with MFN2.

RTNs are a group of evolutionarily conserved proteins residing predominantly in the ER, despite not containing a known ER localization sequence (52,53). RTNs share highly conserved C-terminal reticulon homology domain (RHD), but their N-terminal domains are divergent in length and sequence. The N-terminal domain of RTN1A (isoform A, the longest form) might have a specific role in bridging ER-mitochondria in addition to formation of tubular ER given that RTN1C and RTN3B (shorter forms of RTNs among those tested) showed minimal effect on induction of ER-mitochondria contacts (see Fig. 4C and 4D). Indeed, our data showed the N-terminus (1-568 a.a) of RTN1A has a functional role in coupling EMCs. This result suggests that RTN1A has several functions in its N-terminus

beyond its conserved role in ER shaping. Differential up and down-regulation of RTNs have been linked to neurodegenerative diseases (e.g. Alzheimer's disease, amyotrophic lateral sclerosis, multiple sclerosis, as well as hereditary spastic paraplegia) (62-64). RTN1A has been implicated in the onset of several neurodegenerative diseases, however, what role at plays is unknown (62,65). Disease-linked mutations in RTN1A, specifically in its N-terminus, have not been reported. RTN1A appears to be overexpressed in some chronic kidney diseases, which is thought to increase ER stress (66). Since ER-mitochondria contacts are linked to ER-stress, the unfolded protein response and the formation of autophagosomes, we speculate that dysregulation of RTN1A expression might possibly be related to the onset of the disease. Although further studies are required to elucidate the exact function of RTN1 in EMCs, we suggest that dysregulation of EMCs caused by the ER-shaping protein RTN1A might underlie several neurodegenerative diseases.

The microsomal fraction we used in this study includes vesicle-like artifacts re-formed from pieces of the endoplasmic reticulum (ER) but also membrane vesicles formed from any membrane structure that was soluble after centrifugation. Because the artificial vesicles could be formed with pieces of membrane derived not only from ER, but mitochondria, Golgi, plasma membrane, nuclear envelope, etc, thus the microsomal fraction we obtained is heterogeneous. We adopted the terminology first used when the protocol was first published to avoid any confusion (67).

Interestingly, the cellular component (CC) analysis significantly clustered membrane enclosed organelles including endoplasmic reticulum, mitochondria, lysosomes, exosomes and nuclei. These data suggest mitochondria make contacts with many other organelles, as expected, and the proteins on them can be mapped by Mit-APEX at the moment they come in close proximity.

CC analysis also identified microtubule components, which are likely due to the association of mitochondrial and microtubules for regulation of mitochondrial motility and fusion/fission. Interestingly, ribosome, ribonucleoprotein complex and translation initiation complex were enriched, implying that protein translation activity is also closely related to the outer mitochondrial membrane. Gene set enrichment analysis using Funrich clustered the majority of proteins into membrane bound compartments indicating that mitochondria establish contacts with many different organelles. Previous studies support these results. For example, ER-mitochondrial contacts have been most extensively studied and linked to Ca^{2+} and lipid exchange, intracellular trafficking of ER and mitochondria, ER stress response, autophagy, mitochondrial biogenesis, and inflammasome formation (5-7,10,34,68-71). Peroxisomes and mitochondria functionally and physically interact to maintain lipid homeostasis through β-oxidation of fatty acids and scavenging reactive oxygen species (72,73). Mitochondria are also known to form stable contacts with Golgi and the nuclear envelope (74,75). Although little is known regarding mitochondria and plasma membrane contacts, the Num1/Mdm36 complex was discovered as tethering complex in yeast (17,76). Interestingly, our screen identified stromal interaction molecule 1 (STIM1), which is involved in regulation of store-operated Ca^{2+} entry (SOCE) at ER-PM junctions. This raises the question whether mitochondria might have a role in SOCE (13).

In conclusion, we have successfully applied proximity labeling by Mit-APEX to discover candidate proteins localizing at the contact sites between mitochondrial and other organelles. We have identified and demonstrated that RTN1 increases EMCs. Although we focused on one identified EMC protein, we realize there are many additional candidates derived from our assay, including those localized at the contact sites between mitochondria and other membrane-surfaced organelles such as the Golgi apparatus, peroxisome, and nucleus.

EXPERIMENTAL PROCEDURES

Plasmid constructs

The APEX targeted to the outer mitochondrial membrane was made in pcDNA3.1. APEX (Nat Biotechnol. 2012 Nov; 30(11): 1143–1148). It was fused with the mitochondria-targeting sequence derived from mouse mitochondrial A-kinase anchor protein 1 ((5), AKAP1, residues 34–63: M A I Q L R S L F P L A L P G L L A L L G W W W F F S R K K) using the pcDNA3.1 Directional TOPO Expression Kit to generate pcDNA3.1-Mit- APEX. To detect Mit-APEX, flag-tag (DYKDDDDK) was inserted in between AKAP1 peptide and APEX. RETICULONs (RTN1A; isoform A, RTN2B; isoform B, RTN3B; isoform B) were PCR-amplified using HEK293T cDNA and cloned into pcDNA3 (BamHI, NotI) by GeneArt Seamless cloning method (Thermo Fisher Scientific). RTN1A-DN568 and RTN1A-N568-RTN3 fusion construct was generated using pcDNA3-RTN1A or pcDNA-RTN3B as templates.

Cell culture, SILAC and proximity labeling by Mit-APEX

HEK293T cells (American Type Culture Collection, Manassas, VA) were cultured in Dulbecco's modified Eagle's medium (Invitrogen, CA), with 10% fetal bovine serum (Invitrogen, CA) at 37℃ with 5% CO_2. For SILAC, HEK293T cells were metabotically labeled with Heavy L-arginine and L-lysine using SILAC Protein Quantitation Kits (ThermoFisher Scientific, DMEM). The labeling efficiency was assessed by mass spectrometry before experiments were performed. Fully labeled HEK293T cells were cultured at 37℃ with 5% CO_2. For biotin-labeling of proteins, cells (5 x 10^6/100 mm dish x 4) were plated and transfected with pcDNA3-Mit-APEX using PEI (Ratio of DNA:PEI = 1:3, Polysciences, PA). After 24 hrs in culture the cells were incubated with Biotin-Phenol (500 μM) for 30 min at 37℃, and then treated with 1 mM H_2O_2 for 1 min at room temperature (RT). The biotinylation reaction was quenched by replacing medium with PBS containing 10 mM Na-azide, 10 mM Na-ascorbate, and 5 mM Trolox. After biotinylation, equal numbers of cells were mixed and subjected to biochemical fractionation to collect microsomes and reduce the number of nonspecifically labeled proteins. Microsomal fractionation was performed as previously described (Nat Protoc. 2009;4(11):1582-90). In brief, HEK293 cell homogenate (supernatant) was centrifuged as following: spun at 600 x g for 5 min at 4℃ (two times), at 7,000 x g for 10 min at 4℃ (two times), at 10,000 x g at 4℃, 100,000 x g for 1 hr at 4℃ and the pellet was collected as the microsomal fraction. The isolated microsomal fraction was lysed in RIPA buffer (20 mM Hepes, pH7.4, 150 mM NaCl, 5% glycerol, 1% NP-40, 0.5% Deoxycholic acid, 0.1% SDS, 0.5 mM EDTA, 1.5 mM $MgCl_2$, and protease inhibitors) and centrifuged at

13,000 rpm for 10 min at 4 ℃. The cleared supernatant was incubated with streptavidin magnetic beads (ThermoFisher Scientific) for 1 hr at 4 °C. The beads were subsequently washed three times with RIPA buffer (5 min each time), RIPA + 1 M NaCl, RIPA, 2 M Urea in 10 mM Tris-HCl, pH 8.0, and finally three times with TBS. The beads were dried and stored at -80℃ before mass spectrometric analysis.

LC-MS/MS

Biotinylated targets of SILAC-encoded Mit-APEX pull-downs were digested directly on streptavidin beads and resulting tryptic peptides were sequentially purified by reverse-phase and strong cation exchange batch-mode chromatography. Peptides were separated on a 50 cm analytical column packed with 5 um Monitor tC18 beads using a 60-min gradient from 99% solvent A (0.2 M Acetic acid in water) to 35% solvent B (0.2 M Acetic acid in acetonitrile). Eluted peptides were directly injected into a Q-Exactive HF mass spectrometer (Thermo, Waltham, MA) equipped with a Digital PicoView electrospray source platform (New Objective, Woburn, MA) (Ficarro et al., 2009 PMID: 19331382). The spectrometer was operated in data dependent mode where the top 10 most abundant ions in each MS scan (resolution 240.000, isolation width = 1.5 Da) were subjected to HCD fragmentation (30% normalized collision energy). Dynamic exclusion was enabled with a repeat count of 1 and exclusion duration of 15 seconds. ESI voltage was set to 3.8 kV. The lock-mass function was enabled during MS acquisition and set to recalibrate MS1 scans using the background ion $(Si(CH_3)_2O)_6$ at m/z 445.12 +/- 5 ppm.

MS spectra were converted into a Mascot generic file format (.mgf) using multiplierz scripts (Askenazi et al., 2009; Parikh et al., 2009 PMID: 19874609, PMID: 19333238). Spectra were searched using Mascot (version 2.4) against three appended databases consisting of: i) human protein sequences (downloaded from RefSeq on 07/11/2011); ii) common lab contaminants and iii) a decoy database generated by reversing the sequences from these two databases. Precursor tolerance was set to 10 ppm and product ion tolerance to 0.02 Da. Search parameters included trypsin specificity, up to 2 missed cleavages, fixed carbamidomethylation (C, +57 Da) and variable oxidation (M, +16 Da) with the SILAC quantitation method set to account for differentially labeled lysine (K, +6) and arginine (R, +10). Peptide spectral matches to the reverse database were used to limit the global False Discovery Rate to 1%. The intensity of each SILAC isotope for a given peptide feature was retrieved using custom mutliplierz scripts. The local noise intensity was used to impute isotopes missing from a peptide feature. Protein enrichment ratios were calculated by summing the SILAC intensities of their constituent peptides. Raw mass spectrometry data files have been archived at: ftp://massive.ucsd.edu/MSV000081174.

Split renilla luciferase complementation assay

For the split renilla luciferase complementation assay (22), HEK293T cells (4×10^5/well) were plated in a 12-well culture plate the day before transfection. Expression constructs, pcDNA3-Mit-NRluc91 and pcDNA3-CRluc92-ER were co-transfected with expression constructs encoding RTN1A, RTN2B or RTN3B using PEI (1:4 DNA:PEI ratio, Polysciences, PA). Empty control- and Reep1 expression-vector were used as negative

and positive controls respectively. The cells were re-split into 96-well plate (4 x 10^4/well, Corning; white-wall plate, product #3610) 6 hr post-transfection and further incubated for 18 hours. Twenty four hours post-transfection, Enduren live cell substrate (Promega) was added to the culture media. The cells were further incubated at CO_2 incubator for 2-3 hr and luminescence was measured by POLARstar Omega microplate reader (BMG LABTECH).

Immunofluorescent staining

After transfecting HeLa cells with pcDNA3.1-Mit-APEX and incubating for 24 hr the cells were fixed with 4% paraformaldehyde for 10 min at room temperature (RT), rinsed with PBS, and permeabilized with 0.2% triton X-100 in PBS for 5 min. After blocking in 10% goat serum in PBS, cells were incubated with primary antibodies (Sigma, mouse monoclonal anti-flag M2, 1:500; Santa Cruz Biotechnology, rabbit polyclonal anti-Tom20, 1:500) for 1 hr at RT. After PBS washing three time for 5 min each, secondary anti-mouse Alexa-fluor 488 or anti-rabbit Alexa-fluor 594 (Invitrogen), were incubated for 1 hour at RT. Images were captured with Zeiss Zen Pro software using a Hamamatsu ORCA-Flash4.0 camera attached to a Zeiss Observer Z1 inverted microscope.

Western blotting and silver staining

For western blotting, molecular weight marker (PageRuler plus prestained protein ladder, ThermoFisher Scientific) were included with each gel. Whole cell extract or fractionated protein samples in RIPA buffer were subjected to 4-15% SDS-PAGE (Bio-Rad, Mini-PROTEAN® Precast Gels) and blotted on PVDF membrane (Bio-Rad,Trans-Blot® Turbo™ Mini PVDF Transfer Packs) using Trans-Blot® Turbo™ Transfer System (Bio-Rad). The blotted membrane was soaked in 100% methanol for 30 second and dried completely. Primary antibody (Abcam, Rtn1, ab83049), IP3R-II (A-5), BAP31 (D-6); Novus Biologicals, VAP-B Antibody) was next applied for 1 hr at RT, rinsed three time for 5 min in TBST (Tris buffered saline with 0.5% Tween 20), and incubated with secondary antibody for 1 hr at RT. Membranes were rinsed in TBST containing 1 M NaCl and TBST. Blots were developed using ECL kit (SuperSignal West Pico- or Femto Chemiluminescent Substrate, Thermo Scientific) and scanned using ChemiDoc MP imaging system (Bio-Rad). For silver staining, protein eluates from streptavidin magnetic beads were separated in 4-15% SDS-PAGE gel and stained with SilverQuest™ Silver Staining Kit (Thermo Fisher Scientific) according to manufacturer's instruction.

Functional enrichment analysis

FunRich (Functional Enrichment analysis tool) was used for analyzing SILAC/LC-MSMS results.

Statistical analysis

All statistical analyses were done in Prism software using 2-tailed unpaired Student's t-test. All graphs are plotted as mean ± the standard error of the mean (SEM).

Acknowledgments

This work was supported by the Cotran endowment fund (Jeffrey A. Golden).

Conflict of interest

The authors declare that they have no conflicts of interest with the contents of this article.

Author contributions

IT.C., Y.L. and G.C. designed the experiment. G.A. and J.A.M. conducted LC/MS-MS analysis. IT.C. performed all other experiments and data analysis, and wrote manuscript. J.A.G. supervised research and revised manuscript. All authors reviewed the results and approved the final version of the manuscript.

References

1. Helle, S. C., Kanfer, G., Kolar, K., Lang, A., Michel, A. H., and Kornmann, B. (2013) Organization and function of membrane contact sites. *Biochim Biophys Acta* **1833**, 2526-2541
2. Schrader, M., Godinho, L. F., Costello, J. L., and Islinger, M. (2015) The different facets of organelle interplay-an overview of organelle interactions. *Front Cell Dev Biol* **3**, 56
3. Eisenberg-Bord, M., Shai, N., Schuldiner, M., and Bohnert, M. (2016) A Tether Is a Tether Is a Tether: Tethering at Membrane Contact Sites. *Dev Cell* **39**, 395-409
4. Phillips, M. J., and Voeltz, G. K. (2016) Structure and function of ER membrane contact sites with other organelles. *Nat Rev Mol Cell Biol* **17**, 69-82
5. Csordas, G., Renken, C., Varnai, P., Walter, L., Weaver, D., Buttle, K. F., Balla, T., Mannella, C. A., and Hajnoczky, G. (2006) Structural and functional features and significance of the physical linkage between ER and mitochondria. *J Cell Biol* **174**, 915-921
6. Szabadkai, G., Bianchi, K., Varnai, P., De Stefani, D., Wieckowski, M. R., Cavagna, D., Nagy, A. I., Balla, T., and Rizzuto, R. (2006) Chaperone-mediated coupling of endoplasmic reticulum and mitochondrial Ca2+ channels. *J Cell Biol* **175**, 901-911
7. Hayashi, T., Rizzuto, R., Hajnoczky, G., and Su, T. P. (2009) MAM: more than just a housekeeper. *Trends Cell Biol* **19**, 81-88
8. Bravo, R., Vicencio, J. M., Parra, V., Troncoso, R., Munoz, J. P., Bui, M., Quiroga, C., Rodriguez, A. E., Verdejo, H. E., Ferreira, J., Iglewski, M., Chiong, M., Simmen, T., Zorzano, A., Hill, J. A., Rothermel, B. A., Szabadkai, G., and Lavandero, S. (2011) Increased ER-mitochondrial coupling promotes mitochondrial respiration and bioenergetics during early phases of ER stress. *J Cell Sci* **124**, 2143-2152
9. Rowland, A. A., and Voeltz, G. K. (2012) Endoplasmic reticulum-mitochondria contacts: function of the junction. *Nat Rev Mol Cell Biol* **13**, 607-625
10. Lewis, S. C., Uchiyama, L. F., and Nunnari, J. (2016) ER-mitochondria contacts couple mtDNA synthesis with mitochondrial division in human cells. *Science* **353**, aaf5549
11. Stefan, C. J., Manford, A. G., and Emr, S. D. (2013) ER-PM connections: sites of information transfer and inter-organelle communication. *Curr Opin Cell Biol* **25**, 434-442
12. Henne, W. M., Liou, J., and Emr, S. D. (2015) Molecular mechanisms of inter-organelle ER-PM contact sites. *Curr Opin Cell Biol* **35**, 123-130
13. Jing, J., He, L., Sun, A., Quintana, A., Ding, Y., Ma, G., Tan, P., Liang, X., Zheng, X., Chen, L., Shi, X., Zhang, S. L., Zhong, L., Huang, Y., Dong, M. Q., Walker, C. L., Hogan, P. G., Wang, Y., and Zhou, Y. (2015) Proteomic mapping of ER-PM junctions identifies STIMATE as a regulator of Ca(2)(+) influx. *Nat Cell Biol* **17**, 1339-1347
14. Mesmin, B., Bigay, J., Moser von Filseck, J., Lacas-Gervais, S., Drin, G., and Antonny, B. (2013) A four-step cycle driven by PI(4)P hydrolysis directs sterol/PI(4)P exchange by the ER-Golgi tether OSBP. *Cell* **155**, 830-843

15. De Matteis, M. A., and Rega, L. R. (2015) Endoplasmic reticulum-Golgi complex membrane contact sites. *Curr Opin Cell Biol* **35**, 43-50
16. Gomez-Navarro, N., and Miller, E. (2016) Protein sorting at the ER-Golgi interface. *J Cell Biol* **215**, 769-778
17. Westermann, B. (2015) The mitochondria-plasma membrane contact site. *Curr Opin Cell Biol* **35**, 1-6
18. Dimmer, K. S., Fritz, S., Fuchs, F., Messerschmitt, M., Weinbach, N., Neupert, W., and Westermann, B. (2002) Genetic basis of mitochondrial function and morphology in Saccharomyces cerevisiae. *Mol Biol Cell* **13**, 847-853
19. Giacomello, M., and Pellegrini, L. (2016) The coming of age of the mitochondria-ER contact: a matter of thickness. *Cell Death Differ* **23**, 1417-1427
20. Schon, E. A., and Area-Gomez, E. (2013) Mitochondria-associated ER membranes in Alzheimer disease. *Mol Cell Neurosci* **55**, 26-36
21. Zampese, E., Fasolato, C., Kipanyula, M. J., Bortolozzi, M., Pozzan, T., and Pizzo, P. (2011) Presenilin 2 modulates endoplasmic reticulum (ER)-mitochondria interactions and Ca2+ cross-talk. *Proc Natl Acad Sci U S A* **108**, 2777-2782
22. Lim, Y., Cho, I. T., Schoel, L. J., Cho, G., and Golden, J. A. (2015) Hereditary spastic paraplegia-linked REEP1 modulates endoplasmic reticulum/mitochondria contacts. *Ann Neurol* **78**, 679-696
23. Nishimura, A. L., Mitne-Neto, M., Silva, H. C., Richieri-Costa, A., Middleton, S., Cascio, D., Kok, F., Oliveira, J. R., Gillingwater, T., Webb, J., Skehel, P., and Zatz, M. (2004) A mutation in the vesicle-trafficking protein VAPB causes late-onset spinal muscular atrophy and amyotrophic lateral sclerosis. *Am J Hum Genet* **75**, 822-831
24. De Vos, K. J., Morotz, G. M., Stoica, R., Tudor, E. L., Lau, K. F., Ackerley, S., Warley, A., Shaw, C. E., and Miller, C. C. (2012) VAPB interacts with the mitochondrial protein PTPIP51 to regulate calcium homeostasis. *Hum Mol Genet* **21**, 1299-1311
25. Kuijpers, M., Yu, K. L., Teuling, E., Akhmanova, A., Jaarsma, D., and Hoogenraad, C. C. (2013) The ALS8 protein VAPB interacts with the ER-Golgi recycling protein YIF1A and regulates membrane delivery into dendrites. *EMBO J* **32**, 2056-2072
26. Wang, B., Heath-Engel, H., Zhang, D., Nguyen, N., Thomas, D. Y., Hanrahan, J. W., and Shore, G. C. (2008) BAP31 interacts with Sec61 translocons and promotes retrotranslocation of CFTRDeltaF508 via the derlin-1 complex. *Cell* **133**, 1080-1092
27. Iwasawa, R., Mahul-Mellier, A. L., Datler, C., Pazarentzos, E., and Grimm, S. (2011) Fis1 and Bap31 bridge the mitochondria-ER interface to establish a platform for apoptosis induction. *EMBO J* **30**, 556-568
28. Cacciagli, P., Sutera-Sardo, J., Borges-Correia, A., Roux, J. C., Dorboz, I., Desvignes, J. P., Badens, C., Delepine, M., Lathrop, M., Cau, P., Levy, N., Girard, N., Sarda, P., Boespflug-Tanguy, O., and Villard, L. (2013) Mutations in BCAP31 cause a severe X-linked phenotype with deafness, dystonia, and central hypomyelination and disorganize the Golgi apparatus. *Am J Hum Genet* **93**, 579-586
29. Niu, K., Xu, J., Cao, Y., Hou, Y., Shan, M., Wang, Y., Xu, Y., Sun, M., and Wang, B. (2017) BAP31 is involved in T cell activation through TCR signal pathways. *Sci Rep* **7**, 44809
30. Paillusson, S., Stoica, R., Gomez-Suaga, P., Lau, D. H., Mueller, S., Miller, T., and Miller, C. C. (2016) There's Something Wrong with my MAM; the ER-Mitochondria Axis and Neurodegenerative Diseases. *Trends Neurosci* **39**, 146-157
31. Volgyi, K., Juhasz, G., Kovacs, Z., and Penke, B. (2015) Dysfunction of Endoplasmic Reticulum (ER) and Mitochondria (MT) in Alzheimer's Disease: The Role of the ER-MT Cross-Talk. *Curr Alzheimer Res* **12**, 655-672
32. Krols, M., van Isterdael, G., Asselbergh, B., Kremer, A., Lippens, S., Timmerman, V., and Janssens, S. (2016) Mitochondria-associated membranes as hubs for neurodegeneration. *Acta Neuropathol* **131**, 505-523

33. Filadi, R., Theurey, P., and Pizzo, P. (2017) The endoplasmic reticulum-mitochondria coupling in health and disease: Molecules, functions and significance. *Cell Calcium*
34. Stoica, R., De Vos, K. J., Paillusson, S., Mueller, S., Sancho, R. M., Lau, K. F., Vizcay-Barrena, G., Lin, W. L., Xu, Y. F., Lewis, J., Dickson, D. W., Petrucelli, L., Mitchell, J. C., Shaw, C. E., and Miller, C. C. (2014) ER-mitochondria associations are regulated by the VAPB-PTPIP51 interaction and are disrupted by ALS/FTD-associated TDP-43. *Nat Commun* **5**, 3996
35. Kornmann, B., Currie, E., Collins, S. R., Schuldiner, M., Nunnari, J., Weissman, J. S., and Walter, P. (2009) An ER-mitochondria tethering complex revealed by a synthetic biology screen. *Science* **325**, 477-481
36. Kornmann, B. (2010) [ERMES, a multifunctional complex connecting endoplasmic reticulum and mitochondria]. *Med Sci (Paris)* **26**, 145-146
37. Michel, A. H., and Kornmann, B. (2012) The ERMES complex and ER-mitochondria connections. *Biochem Soc Trans* **40**, 445-450
38. Martell, J. D., Deerinck, T. J., Sancak, Y., Poulos, T. L., Mootha, V. K., Sosinsky, G. E., Ellisman, M. H., and Ting, A. Y. (2012) Engineered ascorbate peroxidase as a genetically encoded reporter for electron microscopy. *Nat Biotechnol* **30**, 1143-1148
39. Hung, V., Zou, P., Rhee, H. W., Udeshi, N. D., Cracan, V., Svinkina, T., Carr, S. A., Mootha, V. K., and Ting, A. Y. (2014) Proteomic mapping of the human mitochondrial intermembrane space in live cells via ratiometric APEX tagging. *Mol Cell* **55**, 332-341
40. Mick, D. U., Rodrigues, R. B., Leib, R. D., Adams, C. M., Chien, A. S., Gygi, S. P., and Nachury, M. V. (2015) Proteomics of Primary Cilia by Proximity Labeling. *Dev Cell* **35**, 497-512
41. Rhee, H. W., Zou, P., Udeshi, N. D., Martell, J. D., Mootha, V. K., Carr, S. A., and Ting, A. Y. (2013) Proteomic mapping of mitochondria in living cells via spatially restricted enzymatic tagging. *Science* **339**, 1328-1331
42. Chen, C. L., Hu, Y., Udeshi, N. D., Lau, T. Y., Wirtz-Peitz, F., He, L., Ting, A. Y., Carr, S. A., and Perrimon, N. (2015) Proteomic mapping in live Drosophila tissues using an engineered ascorbate peroxidase. *Proc Natl Acad Sci U S A* **112**, 12093-12098
43. Hwang, J., and Espenshade, P. J. (2016) Proximity-dependent biotin labelling in yeast using the engineered ascorbate peroxidase APEX2. *Biochem J* **473**, 2463-2469
44. Bendayan, M. (2001) Tech.Sight. Worth its weight in gold. *Science* **291**, 1363-1365
45. Mayer, G., and Bendayan, M. (1997) Biotinyl-tyramide: a novel approach for electron microscopic immunocytochemistry. *J Histochem Cytochem* **45**, 1449-1454
46. Chen, X., Wei, S., Ji, Y., Guo, X., and Yang, F. (2015) Quantitative proteomics using SILAC: Principles, applications, and developments. *Proteomics* **15**, 3175-3192
47. Mann, M. (2006) Functional and quantitative proteomics using SILAC. *Nat Rev Mol Cell Biol* **7**, 952-958
48. Ong, S. E., Blagoev, B., Kratchmarova, I., Kristensen, D. B., Steen, H., Pandey, A., and Mann, M. (2002) Stable isotope labeling by amino acids in cell culture, SILAC, as a simple and accurate approach to expression proteomics. *Mol Cell Proteomics* **1**, 376-386
49. Bendall, S. C., Hughes, C., Stewart, M. H., Doble, B., Bhatia, M., and Lajoie, G. A. (2008) Prevention of amino acid conversion in SILAC experiments with embryonic stem cells. *Mol Cell Proteomics* **7**, 1587-1597
50. Pathan, M., Keerthikumar, S., Ang, C. S., Gangoda, L., Quek, C. Y., Williamson, N. A., Mouradov, D., Sieber, O. M., Simpson, R. J., Salim, A., Bacic, A., Hill, A. F., Stroud, D. A., Ryan, M. T., Agbinya, J. I., Mariadason, J. M., Burgess, A. W., and Mathivanan, S. (2015) FunRich: An open access standalone functional enrichment and interaction network analysis tool. *Proteomics* **15**, 2597-2601
51. Voss, C., Lahiri, S., Young, B. P., Loewen, C. J., and Prinz, W. A. (2012) ER-shaping proteins facilitate lipid exchange between the ER and mitochondria in S. cerevisiae. *J Cell Sci* **125**, 4791-4799

52. Yang, Y. S., and Strittmatter, S. M. (2007) The reticulons: a family of proteins with diverse functions. *Genome Biol* **8**, 234
53. Shibata, Y., Hu, J., Kozlov, M. M., and Rapoport, T. A. (2009) Mechanisms shaping the membranes of cellular organelles. *Annu Rev Cell Dev Biol* **25**, 329-354
54. Wang, S., Tukachinsky, H., Romano, F. B., and Rapoport, T. A. (2016) Cooperation of the ER-shaping proteins atlastin, lunapark, and reticulons to generate a tubular membrane network. *Elife* **5**
55. Powers, R. E., Wang, S., Liu, T. Y., and Rapoport, T. A. (2017) Reconstitution of the tubular endoplasmic reticulum network with purified components. *Nature*
56. Medalia, O., Weber, I., Frangakis, A. S., Nicastro, D., Gerisch, G., and Baumeister, W. (2002) Macromolecular architecture in eukaryotic cells visualized by cryoelectron tomography. *Science* **298**, 1209-1213
57. McGuffee, S. R., and Elcock, A. H. (2010) Diffusion, crowding & protein stability in a dynamic molecular model of the bacterial cytoplasm. *PLoS Comput Biol* **6**, e1000694
58. Prinz, W. A. (2014) Bridging the gap: membrane contact sites in signaling, metabolism, and organelle dynamics. *J Cell Biol* **205**, 759-769
59. Bravo-Sagua, R., Torrealba, N., Paredes, F., Morales, P. E., Pennanen, C., Lopez-Crisosto, C., Troncoso, R., Criollo, A., Chiong, M., Hill, J. A., Simmen, T., Quest, A. F., and Lavandero, S. (2014) Organelle communication: signaling crossroads between homeostasis and disease. *Int J Biochem Cell Biol* **50**, 55-59
60. Hariri, H., Ugrankar, R., Liu, Y., and Henne, W. M. (2016) Inter-organelle ER-endolysosomal contact sites in metabolism and disease across evolution. *Commun Integr Biol* **9**, e1156278
61. Rodriguez-Arribas, M., Yakhine-Diop, S. M., Pedro, J. M., Gomez-Suaga, P., Gomez-Sanchez, R., Martinez-Chacon, G., Fuentes, J. M., Gonzalez-Polo, R. A., and Niso-Santano, M. (2016) Mitochondria-Associated Membranes (MAMs): Overview and Its Role in Parkinson's Disease. *Mol Neurobiol*
62. Mannan, A. U., Boehm, J., Sauter, S. M., Rauber, A., Byrne, P. C., Neesen, J., and Engel, W. (2006) Spastin, the most commonly mutated protein in hereditary spastic paraplegia interacts with Reticulon 1 an endoplasmic reticulum protein. *Neurogenetics* **7**, 93-103
63. Montenegro, G., Rebelo, A. P., Connell, J., Allison, R., Babalini, C., D'Aloia, M., Montieri, P., Schule, R., Ishiura, H., Price, J., Strickland, A., Gonzalez, M. A., Baumbach-Reardon, L., Deconinck, T., Huang, J., Bernardi, G., Vance, J. M., Rogers, M. T., Tsuji, S., De Jonghe, P., Pericak-Vance, M. A., Schols, L., Orlacchio, A., Reid, E., and Zuchner, S. (2012) Mutations in the ER-shaping protein reticulon 2 cause the axon-degenerative disorder hereditary spastic paraplegia type 12. *J Clin Invest* **122**, 538-544
64. Chiurchiu, V., Maccarrone, M., and Orlacchio, A. (2014) The role of reticulons in neurodegenerative diseases. *Neuromolecular Med* **16**, 3-15
65. He, W., Lu, Y., Qahwash, I., Hu, X. Y., Chang, A., and Yan, R. (2004) Reticulon family members modulate BACE1 activity and amyloid-beta peptide generation. *Nat Med* **10**, 959-965
66. Fan, Y., Xiao, W., Li, Z., Li, X., Chuang, P. Y., Jim, B., Zhang, W., Wei, C., Wang, N., Jia, W., Xiong, H., Lee, K., and He, J. C. (2015) RTN1 mediates progression of kidney disease by inducing ER stress. *Nat Commun* **6**, 7841
67. Wieckowski, M. R., Giorgi, C., Lebiedzinska, M., Duszynski, J., and Pinton, P. (2009) Isolation of mitochondria-associated membranes and mitochondria from animal tissues and cells. *Nat Protoc* **4**, 1582-1590
68. Friedman, J. R., Webster, B. M., Mastronarde, D. N., Verhey, K. J., and Voeltz, G. K. (2010) ER sliding dynamics and ER-mitochondrial contacts occur on acetylated microtubules. *J Cell Biol* **190**, 363-375
69. Malhotra, J. D., and Kaufman, R. J. (2011) ER stress and its functional link to mitochondria: role in cell survival and death. *Cold Spring Harb Perspect Biol* **3**, a004424
70. Rainbolt, T. K., Saunders, J. M., and Wiseman, R. L. (2014) Stress-responsive regulation of

mitochondria through the ER unfolded protein response. *Trends Endocrinol Metab* **25**, 528-537
71. Senft, D., and Ronai, Z. A. (2015) UPR, autophagy, and mitochondria crosstalk underlies the ER stress response. *Trends Biochem Sci* **40**, 141-148
72. Lismont, C., Nordgren, M., Van Veldhoven, P. P., and Fransen, M. (2015) Redox interplay between mitochondria and peroxisomes. *Front Cell Dev Biol* **3**, 35
73. Wanders, R. J., Waterham, H. R., and Ferdinandusse, S. (2015) Metabolic Interplay between Peroxisomes and Other Subcellular Organelles Including Mitochondria and the Endoplasmic Reticulum. *Front Cell Dev Biol* **3**, 83
74. Dolman, N. J., Gerasimenko, J. V., Gerasimenko, O. V., Voronina, S. G., Petersen, O. H., and Tepikin, A. V. (2005) Stable Golgi-mitochondria complexes and formation of Golgi Ca(2+) gradients in pancreatic acinar cells. *J Biol Chem* **280**, 15794-15799
75. Prachar, J. (2003) Intimate contacts of mitochondria with nuclear envelope as a potential energy gateway for nucleo-cytoplasmic mRNA transport. *Gen Physiol Biophys* **22**, 525-534
76. Ping, H. A., Kraft, L. M., Chen, W., Nilles, A. E., and Lackner, L. L. (2016) Num1 anchors mitochondria to the plasma membrane via two domains with different lipid binding specificities. *J Cell Biol* **213**, 513-524.

Table 1.

Gene symbol	Protein name	Gene symbol	Protein name
AIMP1	Aminoacyl tRNA synthase complex-interacting multifunctional protein 1	NPLOC4	Nuclear protein localization protein 4 homolog
ANXA7	Annexin A7	NSDHL	Sterol-4-alpha-carboxylate 3-dehydrogenase
ARL6IP5	PRA1 family protein 3	OSBPL8	Oxysterol-binding protein-related protein 8
ATL2	Atlastin-2	P4HB	Protein disulfide-isomerase
BCAP31	B-cell receptor-associated protein 31	PGRMC1	Membrane-associated progesterone receptor component 1
CANX	Calnexin	PDIA4	Protein disulfide-isomerase A4
CAST	Calpastatin	PJA2	E3 ubiquitin-protein ligase Praja-2
CDKAL1	Threonylcarbamoyladenosine tRNA methylthiotransferase	PKD2	Polycystin-2
CISD2	CDGSH iron-sulfur domain-containing protein 2	PRDX4	Peroxiredoxin-4
CLCC1	Chloride channel CLIC-like protein 1	PTPN1	Tyrosine-protein phosphatase non-receptor type 1
CLTC	Clathrin heavy chain 1	RAB1A	Ras-related protein Rab-1A
CNBP	Cellular nucleic acid-binding protein	RPS3A	40S ribosomal protein S3a
COMT	Catechol O-methyltransferase	RTN1	Reticulon-1
COPE	Coatomer subunit epsilon	RTN3	Reticulon-3
CPD	Carboxypeptidase D	SACM1L	Phosphatidylinositide phosphatase SAC1
CYB5R3	NADH-cytochrome b5 reductase 3	SAR1B	GTP-binding protein SAR1b
DDRGK1	DDRGK domain-containing protein 1	SCAPER	S phase cyclin A-associated protein in the endoplasmic reticulum
DLG1	Disks large homolog 1	SCD	Stearoyl-CoA desaturase
EEF1B2	Elongation factor 1-beta	SEC13	Protein SEC13 homolog
EEF1D	Elongation factor 1-delta	SEC22B	Vesicle-trafficking protein SEC22b
EEF1G	Elongation factor 1-gamma	SEC23A	Protein transport protein Sec23A
ERP29	Endoplasmic reticulum resident protein 29	SEC23B	Protein transport protein Sec23B
ERP44	Endoplasmic reticulum resident protein 44	SEC24C	Protein transport protein Sec24C
ESYT1	Extended synaptotagmin-1	SEC24D	Protein transport protein Sec24D
FKBP8	Peptidyl-prolyl cis-trans isomerase FKBP8	SEC31A	Protein transport protein Sec31A
FKBP10	Peptidyl-prolyl cis-trans isomerase FKBP10	SEC61B	Protein transport protein Sec61 subunit beta
FNDC3B	Fibronectin type III domain-containing protein 3B	SEC63	Translocation protein SEC63 homolog
HLA-C	HLA class I histocompatibility antigen	SRPK1	SRSF protein kinase 1
HMGCR	HMG-CoA reductase	SRPRB	Signal recognition particle receptor subunit beta
HNRNPR	Heterogeneous nuclear ribonucleoprotein R	STAU1	Double-stranded RNA-binding protein Staufen homolog 1
HSD17B12	Very-long-chain 3-oxoacyl-CoA reductase	STIM1	Stromal interaction molecule 1
HSP90B1	Endoplasmin	STT3B	Dolichyl-diphosphooligosaccharide--protein glycosyltransferase subunit STT3B
ITGB1	Integrin beta-1	SYNCRIP	Heterogeneous nuclear ribonucleoprotein Q
ITPR2	Inositol 1,4,5-trisphosphate receptor type 2	TBL2	Transducin beta-like protein 2
ITPR3	Inositol 1,4,5-trisphosphate receptor type 3	TMEM43	Transmembrane protein 43
JAGN1	Protein jagunal homolog 1	TMX1	Thioredoxin-related transmembrane protein 1
KTN1	Kinectin	TOR1AIP1	Torsin-1A-interacting protein 1
LAMP2	Lysosome-associated membrane glycoprotein 2	TOR1AIP2	Torsin-1A-interacting protein 2
LRRC59	Leucine-rich repeat-containing protein 59	UBXN4	UBX domain-containing protein 4
MTDH	Protein LYRIC	USO1	General vesicular transport factor p115
NBAS	Neuroblastoma-amplified sequence	USP33	Ubiquitin carboxyl-terminal hydrolase 33
NCSTN	Nicastrin	VAPA	Vesicle-associated membrane protein-associated protein A
NOTCH2	Neurogenic locus notch homolog protein 2	VAPB	Vesicle-associated membrane protein-associated protein B
NPC1	Niemann-Pick C1 protein	VCP	Transitional endoplasmic reticulum ATPase

Figure Legends

Figure 1. Characterization of mitochondria-targeted APEX

(A) Scheme of proximity labeling at ER-mitochondrial contacts (B) Western blot analysis; Mit-APEX (FLAG tag) was expressed in HEK293 cells, and the blot was probed with anti-FLAG antibody. (C) Immunofluorescence images showing Mit-APEX (488 nm in Green), TOM20 (594 nm in red), and merged image (in yellow). Insert represents 3.5x digital enlargement for each image. (D) Activity of Mit-APEX. Biotinylated proteins by Mit-APEX were detected using streptavidin-HRP. (E) HEK293T cells were transfected with pcDNA-Mit-APEX and pilot biotinylation was performed using whole cell lysate. Biotinylated proteins were purified with Streptavidin-magnetic beads and the eluates were run on SDS-PAGE. Proteins blot was probed with antibodies as indicated.

Figure 2. Stable isotope labeling with amino acids in cell culture (SILAC) and purification of biotinylated proteins. (A) Experimental flow chart for SILAC and sample processing prior to LC-MS/MS. (B) Subcellular fractionation of cells after biotinylation. Proportional amount of lysate in each fraction (volume basis) was run on SDS-PAGE and probed against marker proteins as indicated. Crude Mitochondrial and nuclear fractions were separated. Western blot with Streptavidin HRP shows a different pattern of biotin labeling. (C) Silver staining of purified, biotinylated proteins.

Figure3. GO term analysis: proteomic profiling of proteins identified by LC-MS/MS. Quantitative SILAC results from replicates were normalized by quantile method using R software. By applying 2.0-fold cut-off ratio (log base 2) in SILAC quantification, 405 proteins were isolated. Cellular component analysis using Funrich was performed with these protein lists, and Top 15 clusters (p-value < 0.05) were presented. FunRich human database was used for the enrichment analysis.

Figure 4. RETICULON1 (RTN1) enhances ER-Mitochondria contact. (A) Scheme of split renilla luciferase (Split-Rluc8) reconstitution assay. Mit-NRluc and CRluc-ER alone have no expected luciferase activity. However, when in proximity to each other they establish functional complementation, thus assemblying an active luciferase that, in the presence of the Enduren live cell substrate, generates a luminescence product. The level of ER-mitochondria is measured as luminescence by catalytic conversion of Enduren substrate. (B) Western blotting of biotin-phenol labeled ER-mitochondria tethering proteins. Proteins purified using streptavidin magnetic beads after biotin-phenol labeling by Mit-Apex were run on SDS-PAGE and probed with antibodies as indicated. (C) Scheme of RETICULONs used in this study, the numbers correspond to exons. (D) RETICULONs (RTN1A, RTN2B, and RTN3B) increased Split Rluc8 activity, while RTN1C showed no increase. Empty control vector and Reep1 expression vector were used as negative and positive control respectively. ****p<0.0001 and ***p<0.001

(n=3). (E) N-terminal (1-568 a.a) deletion mutant of RTN1A (RTN1A-ΔN568) and the RTN1A N-terminus (1-568 a.a)-RTN3B fusion constructs (RTN1A-N568-RTN3B) were expressed in HEK293 cells and the Split Rluc8 activity was compared between proteins indicated. (F) RTN1A and RTN1A-ΔN568 were co-expressed with Mit-APEX in HEK293 cells, biotin-labeling and purification by streptavidin-beads were performed. The level of proximity labeling efficiency was compared by western blotting.

Figure 1

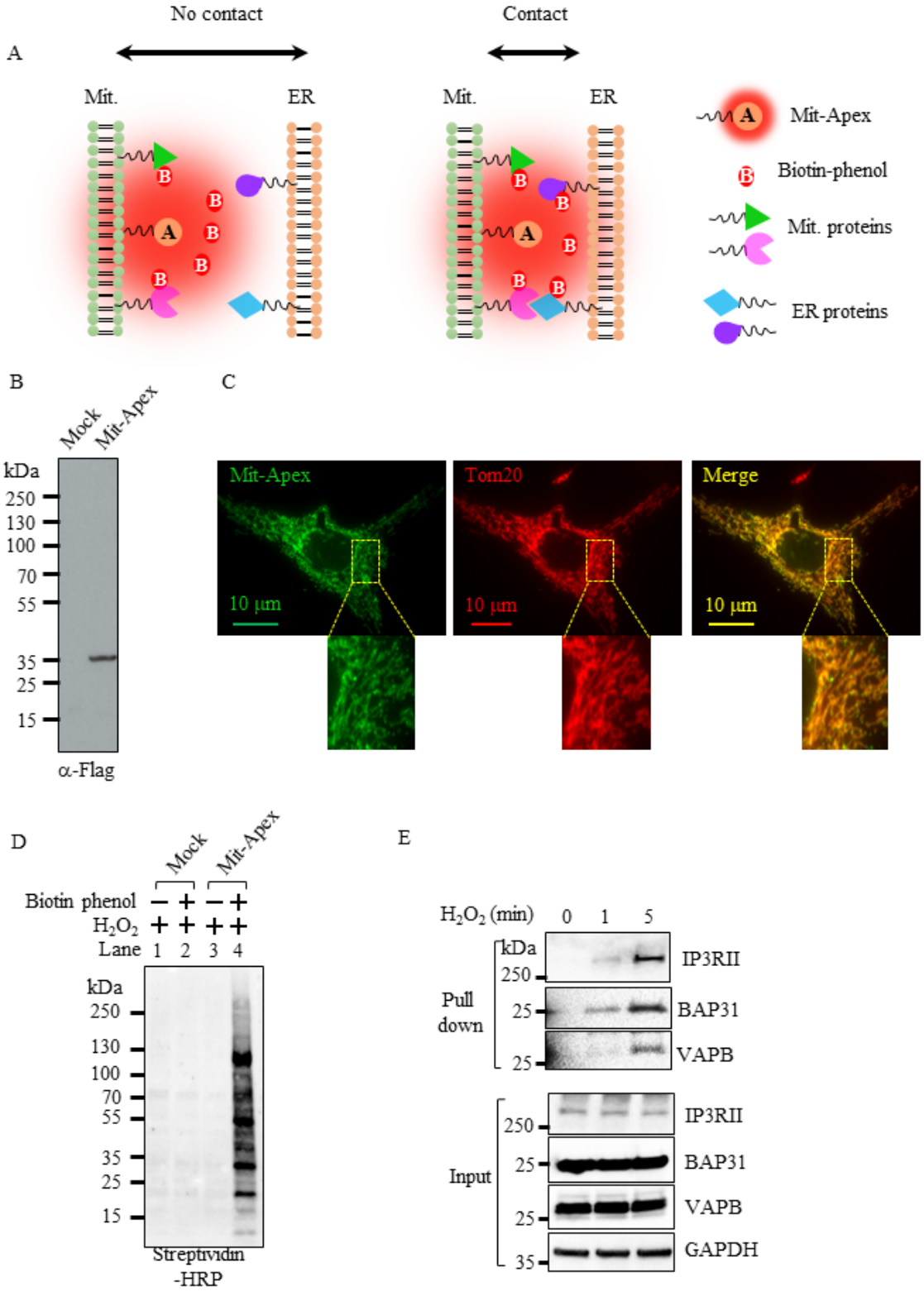

Figure 2

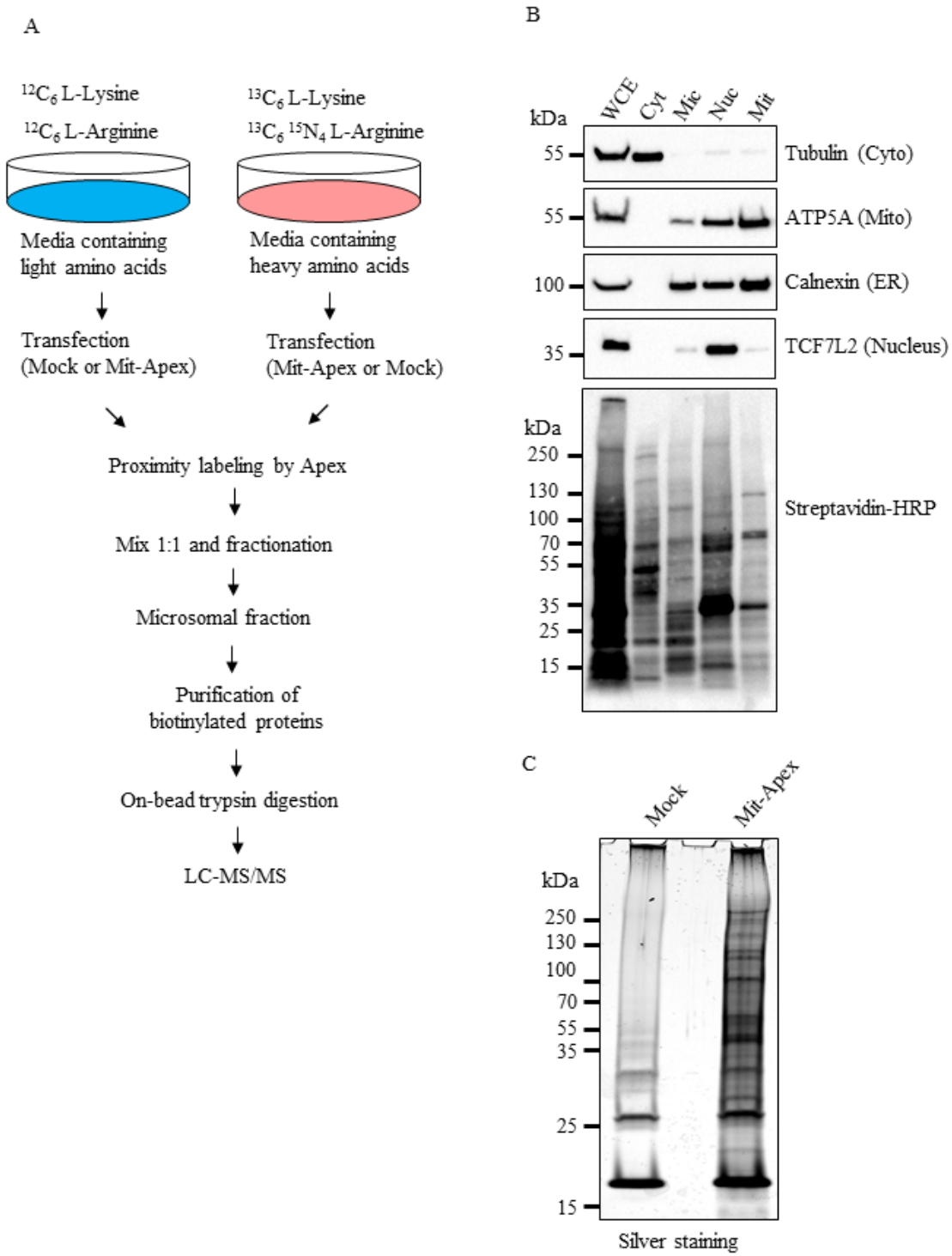

Figure 3

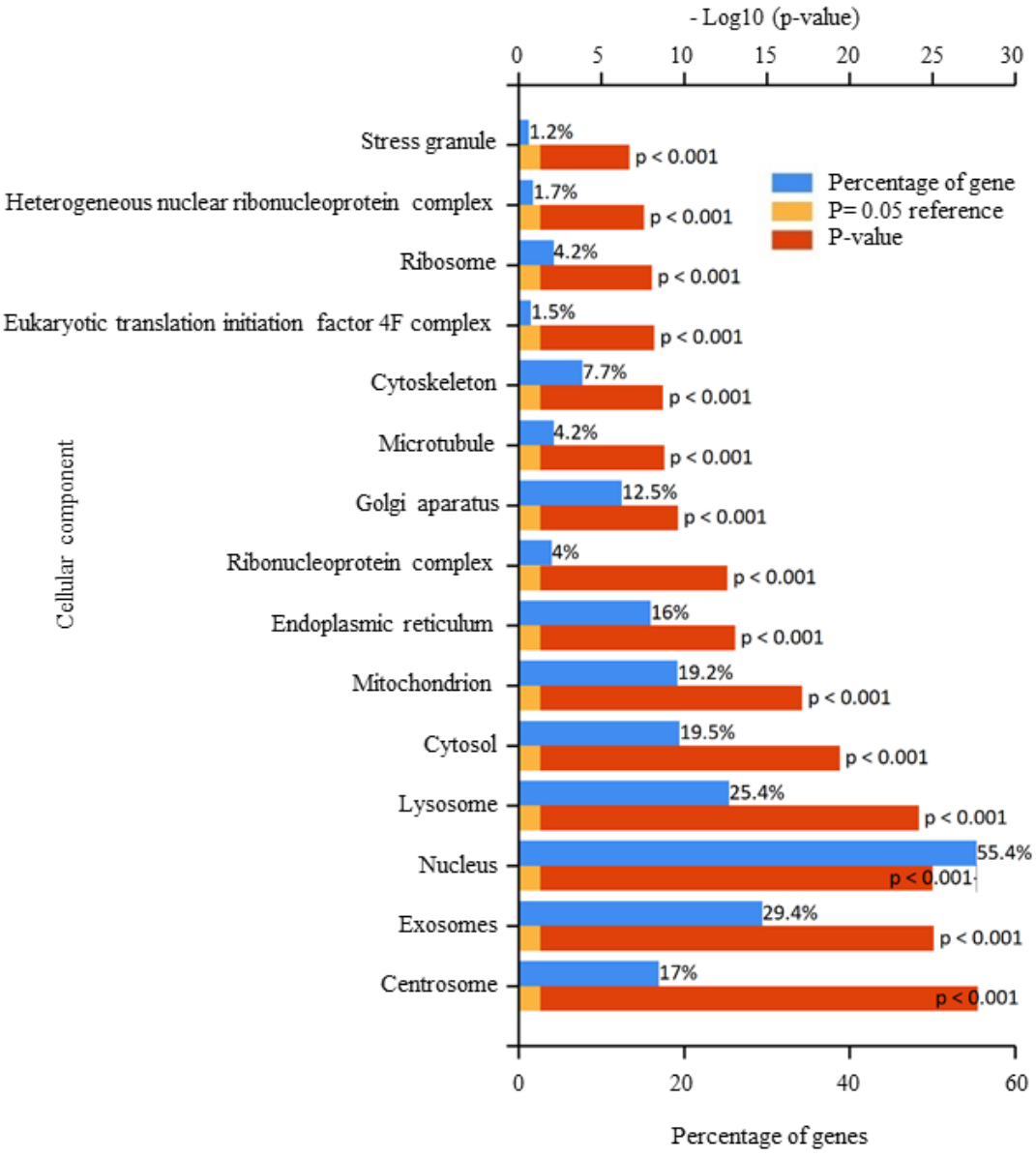

Figure 4

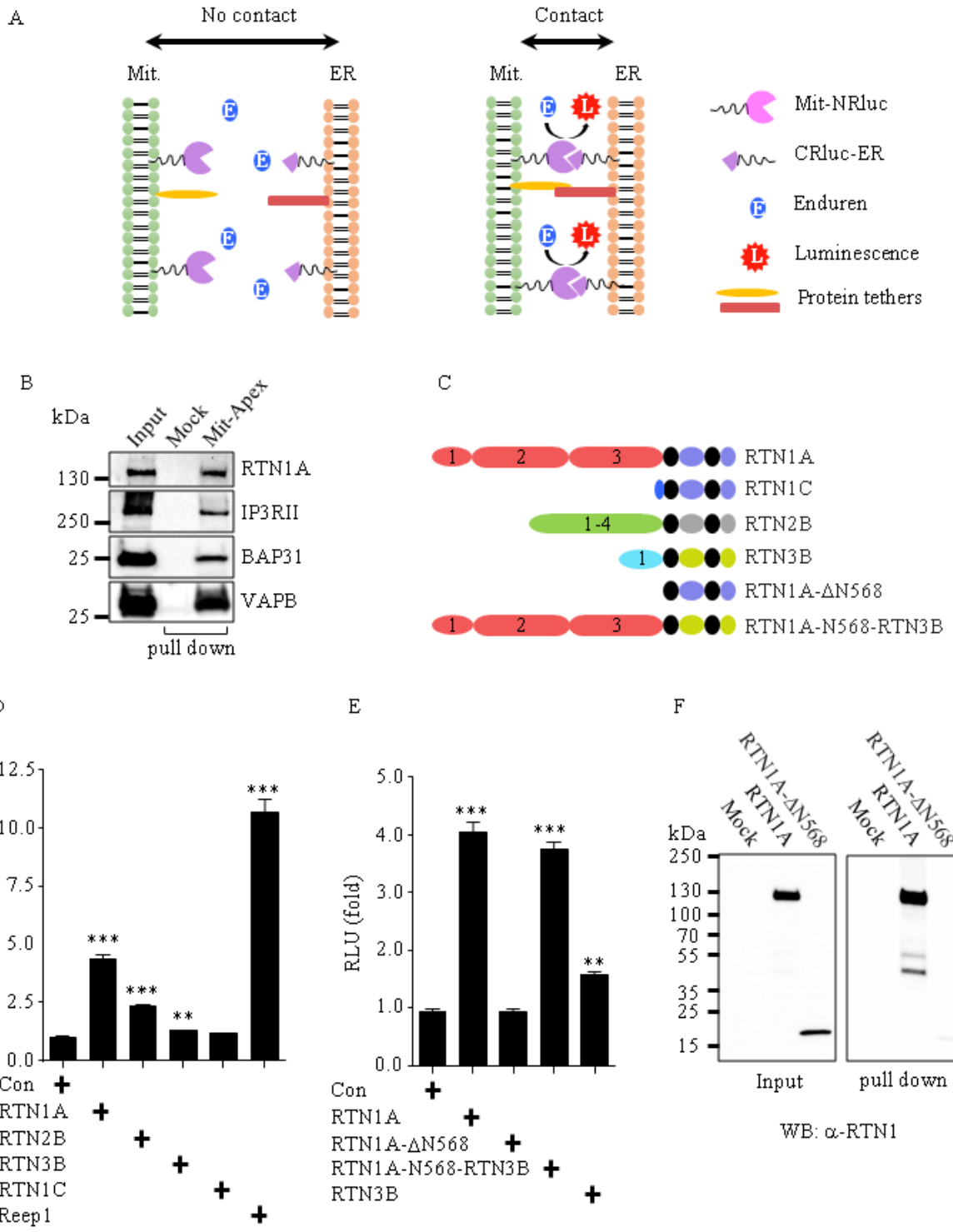

Ascorbate peroxidase proximity labeling coupled with biochemical fractionation identifies promoters of endoplasmic reticulum mitochondrial contacts

Il-Taeg Cho, Guillaume Adelmant, Youngshin Lim, Jarrod A Marto, Ginam Cho and Jeffrey A Golden

J. Biol. Chem. published online July 31, 2017
